2007

Simulations of the Extratropical Transition of Tropical Cyclones: Phasing between the Upper-Level Trough and Tropical Cyclones

Simulations of the Extratropical Transition of Tropical Cyclones: Phasing between the Upper-Level Trough and Tropical Cyclones

ELIZABETH A. RITCHIE

Department of Electrical and Computer Engineering, University of New Mexico, Albuquerque, New Mexico

RUSSELL L. ELSBERRY

Department of Meteorology, Naval Postgraduate School, Monterey, California

(Manuscript received 22 August 2005, in final form 5 May 2006)

ABSTRACT

Whether the tropical cyclone remnants will become a significant extratropical cyclone during the reintensification stage of extratropical transition is a complex problem because of the uncertainty in the tropical cyclone, the midlatitude circulation, the subtropical anticyclone, and the nonlinear interactions among these systems. In a previous study, the authors simulated the impact of the strength of the midlatitude circulation trough without changing its phasing with the tropical cyclone. In this study, the impact of phasing is simulated by fixing the initial position and amplitude of the midlatitude trough and varying the initial position of the tropical cyclone. The peak intensity of the extratropical cyclone following the extratropical transition is strongly dependent on the phasing, which leads to different degrees of interaction with the midlatitude baroclinic zone. Many aspects of the simulated circulation, temperature, and precipitation fields appear quite realistic for the reintensifying and dissipating cases. Threshold values of various parameters in quadrants near and far from the tropical cyclone are extracted that discriminate well between reintensifiers and dissipators. The selection and distribution of threshold parameters are consistent with the Petterssen type-B conceptual model for extratropical cyclone development. Thus, these simulations suggest that phasing between the tropical cyclone and the midlatitude trough is a critical factor in predicting the reintensification stage of extratropical transition.

1. Introduction

The second, or *reintensification,* stage of the extratropical transition (ET) of tropical cyclones (TCs) occurs when a transformed tropical cyclone reintensifies if the midlatitude conditions are favorable for extratropical cyclogenesis, which is usually as part of an interaction with a midlatitude upper-level trough (e.g., DiMego and Bosart 1982; Harr and Elsberry 2000; Klein et al. 2000; Hart and Evans 2001; Sinclair 2002). Klein et al. (2000) noted in their study of 30 western North Pacific ET events that this *reintensification* stage was very dependent on the details of the midlatitude circulation structure and how the transformed tropical cyclone interacted with that midlatitude circulation. In particular, poleward-moving tropical cyclones underwent a variety of reintensification rates. Of those that did significantly reintensify, the ability of forecast models to accurately predict the rate of intensification and future track of the storm was at times poor, with large discrepancies from forecast to forecast even by the same model (P. Harr 2000, personal communication). This led to the Harr and Elsberry (2000) hypothesis that the details of the structure of the transformed tropical cyclone have relatively little influence on the intensification processes; rather, it is the structure of the midlatitude environment that determines the rate and nature of reintensification. If the forecast model poorly handles the timing of the transformed tropical cyclone with the midlatitude environment, a poor reintensification forecast results.

Prior studies of ET (DiMego and Bosart 1982; Sinclair 1993; Foley and Hanstrum 1994; Harr and Elsberry 2000; Harr et al. 2000) have described reintensification of the transformed tropical cyclone in terms of a type-B development following Petterssen and Sme-

Corresponding author address: Elizabeth Ritchie, University of New Mexico, ECE Building, Room 125, Albuquerque, NM 87131. E-mail: ritchie@ece.unm.edu

DOI: 10.1175/MWR3303.1

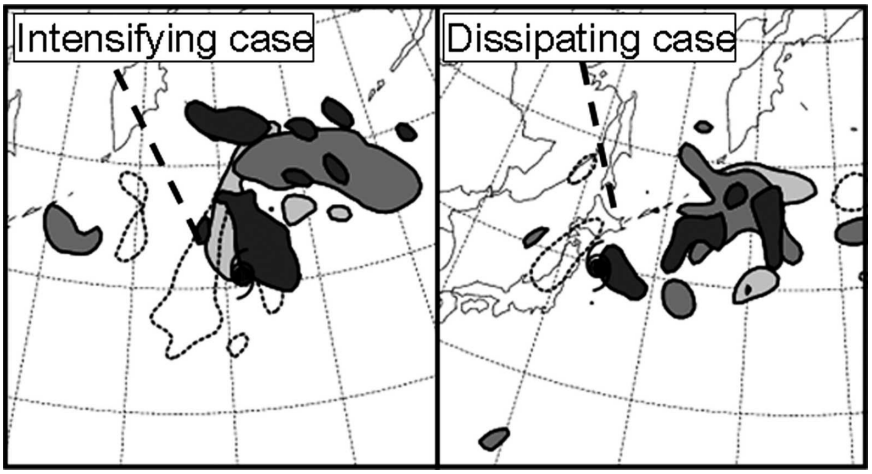

FIG. 1. Critical values of the Peterssen development parameters (see text for details) of upper-level divergence (light gray shading), low-level temperature advection (warm—medium gray shading, cold—dashed contouring), and midlevel positive vorticity advection (dark gray shading) plotted for an intensifying and dissipating case at the end of stage 1 of the ET.

bye (1971). In this context, low-level cyclone development occurs when an area of midlevel positive vorticity advection (PVA) becomes superposed over a low-level frontal region, allowing low-level thermal advection to contribute significantly to an increase in low-level vorticity. When the thermal field is distorted by the low-level tropical cyclone circulation, as may occur during transformation of a tropical cyclone (Klein et al. 2000), the thermal contribution becomes significant (e.g., Keyser et al. 1988; Petterssen 1956). In this framework, the phasing (or relative spatial location) of the tropical cyclone remnants with the upper-level trough clearly should be the key factor in determining whether the low- and upper-level components of type-B development are properly superposed during the reintensification of the extratropical cyclone. An example is presented in Fig. 1 of how critical the phasing of the tropical cyclone and upper-level trough is to the reintensification of the extratropical system. Figure 1 is a plot superposing critical levels of the three Peterssen development parameters of upper-level divergence $>3 \times 10^{-5}$ s^{-1}, midlevel positive vorticity advection $>20 \times 10^{-10}$ s^{-2}, and low-level temperature advection $>\pm 10 \times 10^{-5}$ K s^{-1} defined in Klein et al. (2002) and discussed in Ritchie and Elsberry (2003). In Fig. 1a, these parameters cover a large area downstream of the trough axis. The tropical cyclone is collocated with these areas and thus is contributing to the potential extratropical intensification. This system goes on to reintensify from 992 to 964 mb in 40 h. In Fig. 1b, the parameters are all collocated although they do not cover as extensive a region as in Fig. 1a. The tropical cyclone remnants are located to the west of this area (and the southward extension of the trough axis) and therefore do not contribute to the extratropical development of the remnant TC. There is no phasing between the tropical cyclone and the upper-level trough, and this case dissipates.

Ritchie and Elsberry (2003) studied the relationship between the strength of the upper-level trough and subsequent reintensification without altering the relative initial locations between the two weather systems. In their idealized simulations, the strength of the upper-level trough had little impact on the peak intensity of the extratropical cyclone, but did impact the rate at which the intensification occurred. Of note was their conclusion that the basic structure of the midlatitude environment may have more to do with the peak intensity of the extratropical cyclone than the strength of the upper-level trough embedded within that environment as their basic environment was the same for all simulations.

The purpose of this study is to continue to investigate the interaction between the midlatitude upper-level trough and the tropical cyclone during the reintensification stage of ET. In particular, the effects of altering the phasing between the upper-level, midlatitude trough and the tropical cyclone are investigated. Following Ritchie and Elsberry (2003), a series of simulations are performed using the Navy's Coupled Ocean–Atmospheric Mesoscale Prediction System (COAMPS) to investigate how different phasing between a midlatitude upper-level trough and the tropical cyclone impact the subsequent reintensification of the extratropical cyclone. As noted in Klein et al. (2002), changing the relative location of the systems by only a small amount

can dramatically affect the subsequent interaction. Specifically, this study differs from that of Klein et al. (2002) and McTaggart-Cowan et al. (2001) in that it directly examines the effect of modifying the phasing between the upper-level trough and the tropical cyclone without changing the specific characteristics of either weather system as an intermediate step to understanding the reintensification stage of the ET of a tropical cyclone.

The structure of the paper will be as follows. A description of the modeling system and experimental setup will be provided in section 2. The consequences of altering the phasing between the upper-level trough and tropical cyclone will be discussed in section 3. A comparison of the major differences that produce dissipating systems as opposed to moderate or strongly reintensifying systems will be provided in section 4. A preliminary parameter identifier for whether a system will dissipate or reintensify is discussed in section 5. The summary and conclusions are provided in section 6.

2. Description of the modeling system

High-resolution idealized simulations of ET will be studied here using only the atmospheric portion of COAMPS (Hodur 1997). The advantage of simulations using such a modeling system is that the varying atmospheric conditions among cases can be controlled.

a. Model description

The COAMPS model employed in the study is described in detail by Hodur (1997). The system is nonhydrostatic, has multiple nested grids, and includes a Kain–Fritsch (Kain and Fritsch 1993) representation of convection, and single-moment prediction of the mixing ratio of vapor, pristine ice, snow, rain, and cloud water for grid-scale saturation (Rutledge and Hobbs 1983). Additional parameterizations include subgrid-scale mixing (Deardorff 1980), surface fluxes (Louis 1979), and a radiation scheme that includes both shortwave and longwave radiative transfer calculations considering both cumulus and stratiform cloud types (Harshvardhan et al. 1987). The primitive equations are solved on a Lambert conformal grid, with a terrain-following σ coordinate in the vertical. The model has 36 layers from $\sigma = 0$ to 1, with the vertical boundaries at 30 km and the surface. Whereas vertical velocity is defined at the interfaces of the model layers, all other variables are carried at the midpoints of the layers. The horizontal grid has an Arakawa–Lamb C staggering of the momentum variables (u and v) with respect to the other variables.

The configuration used for these simulations is the same as that for Ritchie and Elsberry (2003) and are described there. Briefly, the coarse and fine meshes have grid spacings of 81 km and 27 km, respectively. The coarse domain of 87×93 grid points (see Ritchie and Elsberry 2003, their Fig. 1) is large enough to allow an adequate representation of the upper-level midlatitude trough development during the integration. The fine mesh of 124×190 grid points captures the primary structural modifications of the storm as it interacts with the upper-level trough. The coarse grid supplies boundary values to the fine mesh, which in turn feeds information back to the coarse grid after the fine mesh integration step is completed. The two-way interaction ensures that the fine mesh structure is well represented on the coarse mesh. Consequently, only coarse mesh figures will be presented here. Lateral boundary conditions (Perkey and Krietzberg 1976) around the coarse domain force the model-predicted variables near the outer boundary to adjust to the fixed initial values.

b. Experimental setup

The initial environmental wind vertical structure is the same as that used in Ritchie and Elsberry (2003) and is based on composite data of western North Pacific ET cases (Ritchie and Elsberry 2001, step 3 in their Fig. 3). The horizontal variation in the environmental wind is based on a Gaussian distribution that results in a jet in the wind field near 47°N (not shown). Given this wind structure, the corresponding mass and temperature fields are derived to be in geostrophic and hydrostatic balance, with the mean thermal sounding specified as the composite pretropical depression sounding of McBride and Zehr (1981). Although geography is included in figures to help orient the reader, these are idealized simulations in which the entire domain is over ocean. A time-invariant sea surface temperature gradient is specified to match the near-surface air temperature gradient. This is designed so that the specified surface fluxes of moisture and heat do not modify the basic-state near-surface temperature structure through the simulation. The McBride and Zehr (1981) composite vertical profile of relative humidity is specified everywhere so that the meridional temperature gradient implies moist (dry) air to the south (north). A balanced upper-level potential vorticity perturbation with a Gaussian vertical wind structure maximum at 380 mb is then added to this environment to represent the midlatitude upper-level trough. The maximum wind associated with the potential vorticity perturbation is 15 m s^{-1}, which corresponds to the weak trough cases in Ritchie and Elsberry (2003) and results in an upper-level jet streak with a maximum of 50 m s^{-1} at 250 mb.

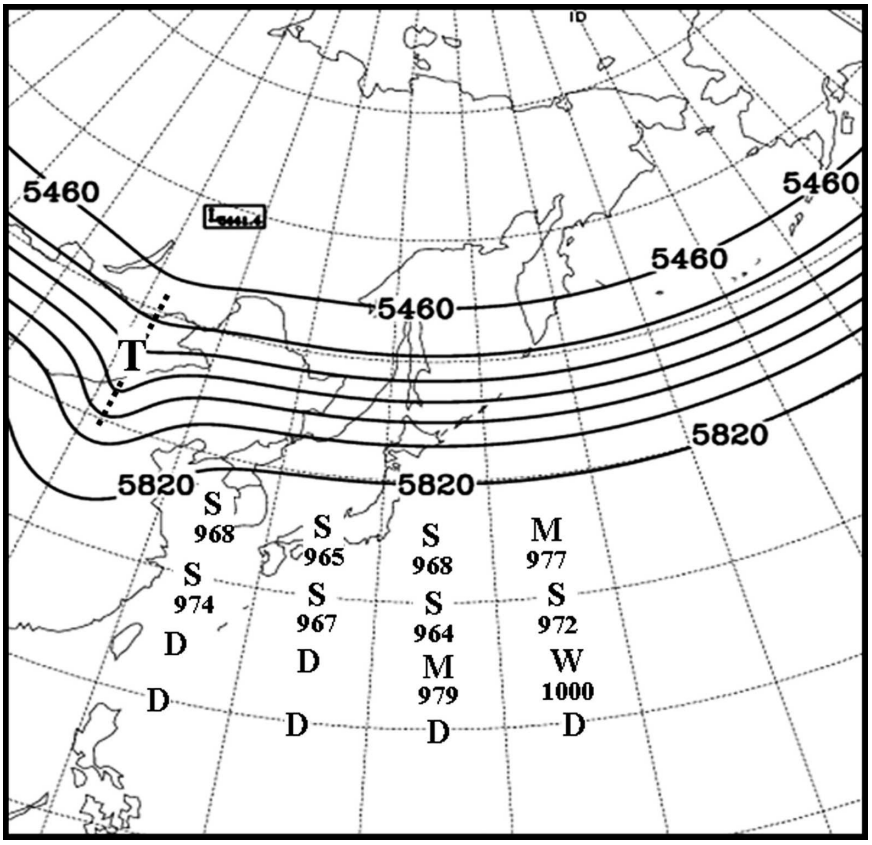

FIG. 2. Schematic indicating the final intensities each extratropical cyclone reached, their classification (S, M, and D), and their initial location relative to the upper-level trough (T). The background field is the 500-mb geopotential height field of the environment without a TC embedded.

The initialization and insertion of the tropical cyclone is the same as in Ritchie and Elsberry (2001, 2003) and Frank and Ritchie (2001). The tropical cyclone is spun up in a quiescent environment based on the McBride sounding until an approximately steady-state intensity of 960 mb is reached and the cloud fields are fully developed. This initial tropical cyclone has a maximum wind of 55 m s^{-1} at a radius of 70 km. The core structure is approximately symmetric with cyclonic winds extending to 50 mb in the core and a maximum temperature anomaly of 12 K at 450 mb (see Fig. 5 in Ritchie and Elsberry 2001). The 300-mb winds turn weakly anticyclonic at 400-km radius.

The initial conditions for 16 simulations are created by inserting the perturbations associated with the tropical cyclone into the environment every 5° latitude–10° longitude in a 4 × 4 grid (Fig. 2). The closest location to the trough is 10°S and 15°E of the trough, and the farthest location is 25°S and 45°E of the trough (Fig. 2). While there are some slight imbalances in the initial flow fields in the vicinity of the storm when the environment is imposed, their effect on the simulated storms is brief and temporary. As described below, the simulated storms develop as would be expected for a tropical cyclone moving into an increasing midlatitude environment, and the asymmetries that develop after the shear is imposed are persistent, indicating that they are quasi-balanced rather than transient phenomena. All simulations are integrated for 192 h. By this time the original trough has advected out of the area of interest, and any subsequent development is due to interaction with the in situ development of a secondary trough.

3. The phasing between the upper-level trough and the tropical cyclone

The evolution of the minimum sea level pressure (SLP) associated with each simulation is shown in Fig. 3. The final pressures can be clustered into three reintensification groups that are similar to those defined by Klein et al. (2000): non/weak (NW: SLP > 1000 mb),

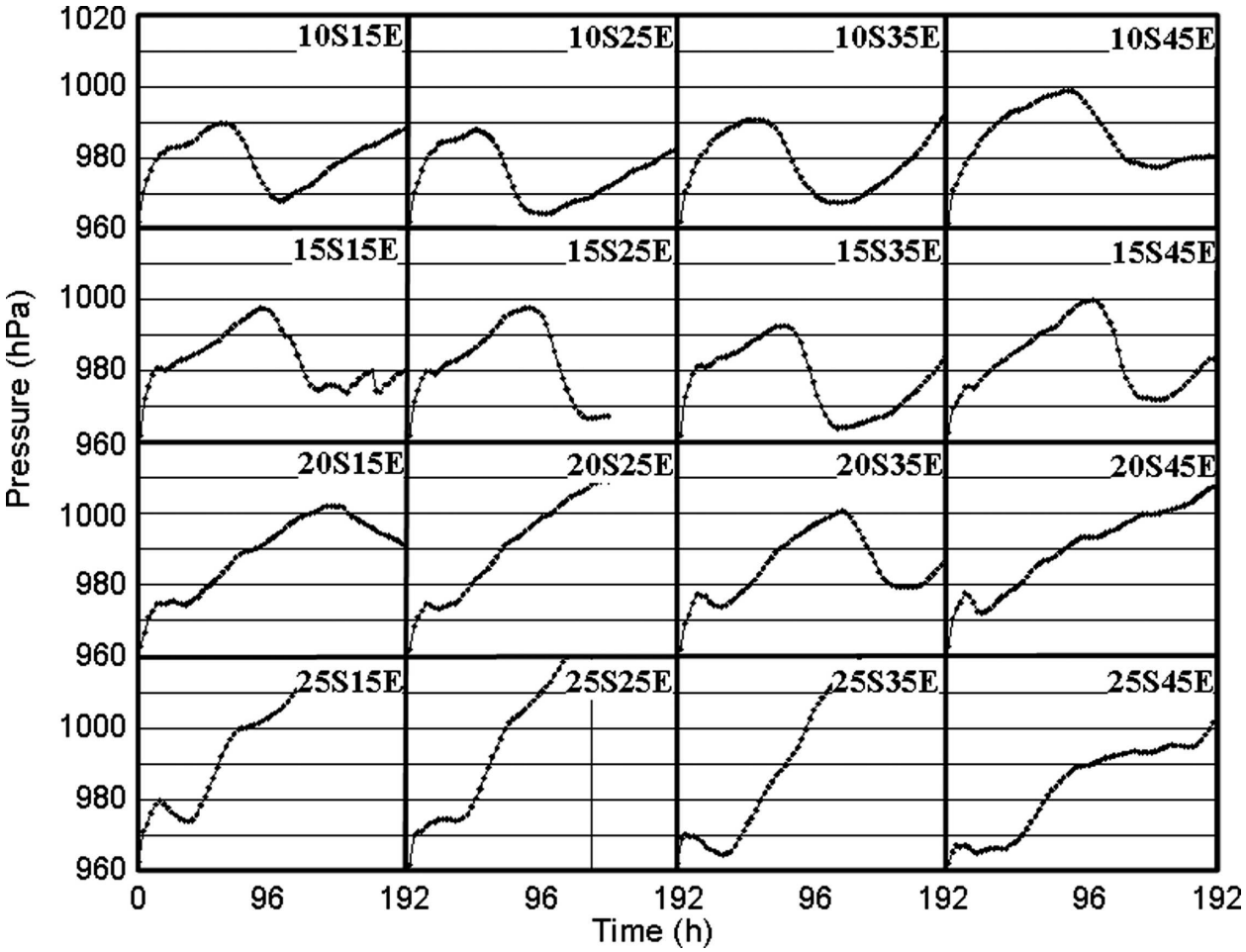

FIG. 3. Time series of the minimum surface pressure for all 16 simulations. Location of the TC relative to the upper-level trough is indicated by the location in the grid.

moderate (M: 975 mb $<$ SLP $<$ 999 mb), and strong (S: SLP $<$ 975 mb) intensifiers. In these idealized simulations, the different evolutions must be due to differences in the interaction between the midlatitude trough and the tropical cyclone arising only from the relative positions in Fig. 2. The peak intensity achieved by the system (Fig. 3) is strongly dependent on the relative positioning of the tropical cyclone and midlatitude trough (Fig. 2). In general, those cases in which the tropical cyclone is initially closest to the baroclinic zone and upper-level trough (within 15° latitude) develop the deepest intensities and those farthest away (20°–25°S of the trough) are more likely to dissipate or only weakly reintensify. However, the reintensification varies with the initial longitudinal position as well.

The reasons for these evolutions may be sought in the tropical cyclone paths relative to the baroclinic zone associated with the upper-level trough. The tropical cyclones initially closest to the baroclinic zone tracked northeast immediately into and across the baroclinic zone (Figs. 4a–h,k), advected by the southwesterly flow ahead of the upper-level trough. The tropical cyclones (Figs. 4i,j,l, and 4m–p) that dissipated had a stronger eastward component to their track. By the time these tropical cyclones approached and crossed the baroclinic zone, the upper-level trough had already passed to the east. Instead of interacting with the trough, these tropical cyclones were advected by the westerlies associated with the background baroclinic zone and moved rapidly eastward as they dissipated in the environmental vertical wind shear.

The seemingly anomalous strong reintensification of the 15°S and 45°E tropical cyclone has a track similar to that of the more northern cases, which is an indication that an interaction between the tropical cyclone and midlatitude trough did in fact occur. Note that the spatial patterning did not apply to the southeastern-most series of simulations. In these cases (Figs. 4l,p), the ini-

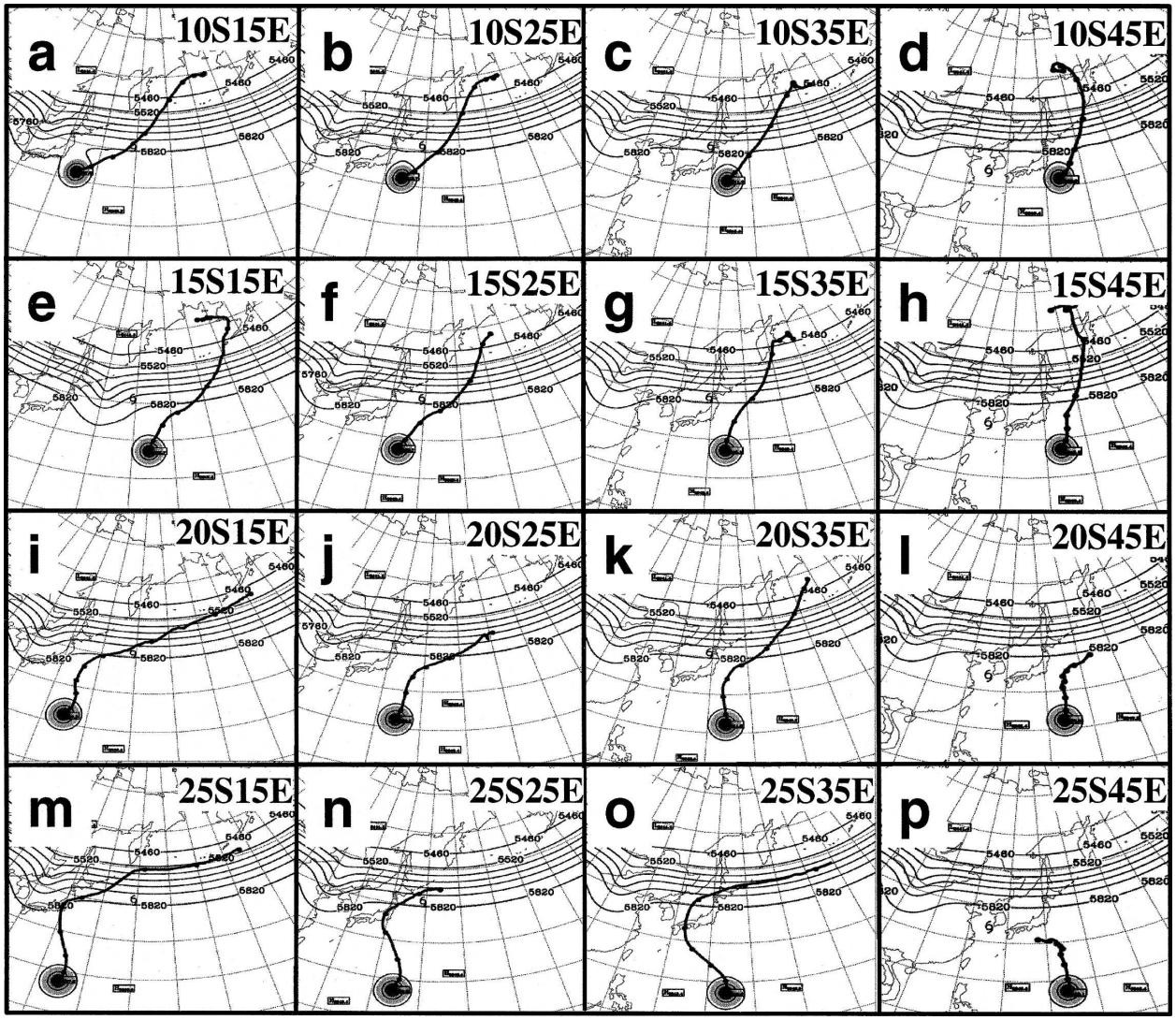

FIG. 4. The 500-mb height fields showing the initial location of the TC relative to the upper-level trough for all 16 simulations. The subsequent track of the minimum surface pressure is superposed.

tial 5 m s^{-1} advection to the northeast added to the tropical cyclone did not advect the tropical cyclone into the midlatitude westerlies before the trough had passed by. These two cases gradually weakened and eventually dissipated through the course of the simulations.

In summary, this dependency on the initial position of the tropical cyclone highlights the complexity of the phasing between the tropical cyclone and trough for future intensification. These results strongly support the conclusions of Klein et al. (2002) that the reintensification or dissipation of the extratropical cyclone is very dependant on the relative locations of the tropical cyclone and midlatitude upper-level trough. In fact, this series of simulations, in concert with the authors' previous research, suggests that the phasing between the tropical cyclone and midlatitude trough may be the single most important factor in accurately predicting future intensification trends of a transitioning cyclone in numerical weather prediction models.

4. Simulated extratropical transition

In this section, two representative simulations are examined in some detail to highlight the main differences that occur between a dissipating tropical cyclone and an intensifying tropical cyclone during extratropical transition.

a. Reintensifiers—Case 15S35E

The 500-mb geopotential height and SLP patterns are presented in Fig. 5 at key stages in the life cycle of

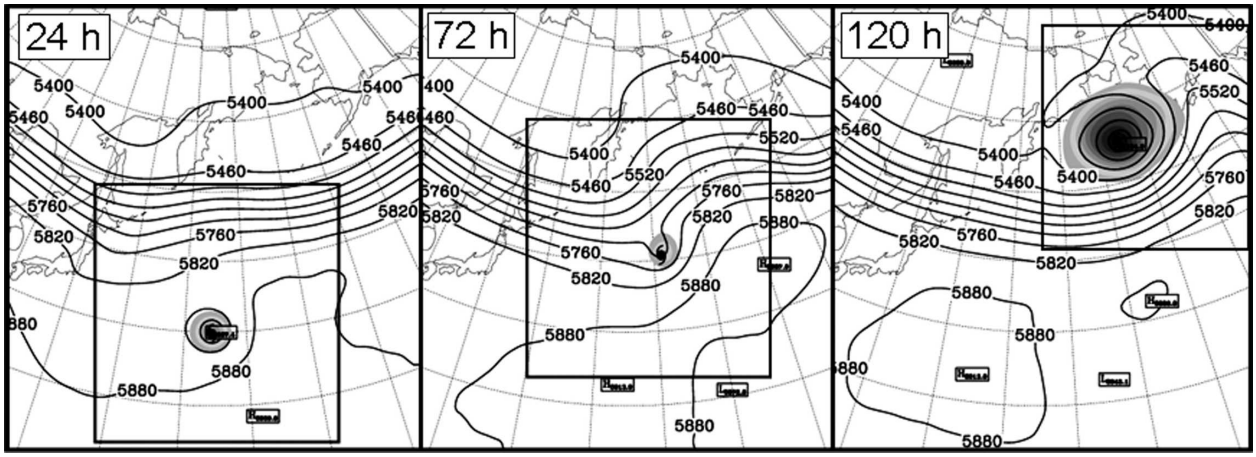

FIG. 5. The 500-mb geopotential height field (contour = 60 m) and SLP (shaded every 4 mb < 1000 mb) for the intensifying case (15S35E): (a) 24 h, (b) end of stage 1, and (c) end of stage 2. The boxes indicate the domains for Figs. 6 and 7.

a reintensifying extratropical transition case. Initially the midlatitude trough and the tropical cyclone are distinct features in the 500-mb height and surface pressure fields (Fig. 5a). Prior to 72 h of integration, the tropical cyclone undergoes transformation or stage 1 of extratropical transition (Klein et al. 2000), and weakens considerably as it approaches the midlatitude baroclinic zone with increasing midlatitude vertical wind shear and lower SSTs (Fig. 3). By 72 h (Fig. 5b), the tropical cyclone has become embedded in the midlatitude trough in the 500-mb fields as an open wave. Although it does still have a distinct surface center in the SLP field, it has filled to almost its highest central SLP, which corresponds to the end of stage 1 of extratropical transition as defined by Klein et al. (2000). Subsequent to 72 h of integration, the system enters stage 2 of extratropical transition (Klein et al. 2000) and begins to reintensify (Fig. 3). During this time, the system is tilted to the west with height (not shown) similar to many documented cases of ET (e.g., DiMego and Bosart 1982; Klein et al. 2002; Sinclair 1993; Thorncroft and Jones 2000). The extratropical cyclone reaches the end of stage 2 as defined by Klein et al. (2000) when the extratropical cyclone is most intense (964 mb) and is beginning to occlude (Fig. 5c).

The 850-mb temperature maps that correspond to the boxed areas in Fig. 5 are presented in Fig. 6. Initially the temperatures exceeding 22°C are concentrated in the core of the TC (Fig. 6a). The strong temperature gradient associated with the baroclinic zone is to the north of the TC. By the end of stage 1, the tropical cyclone has moved into the baroclinic zone and the

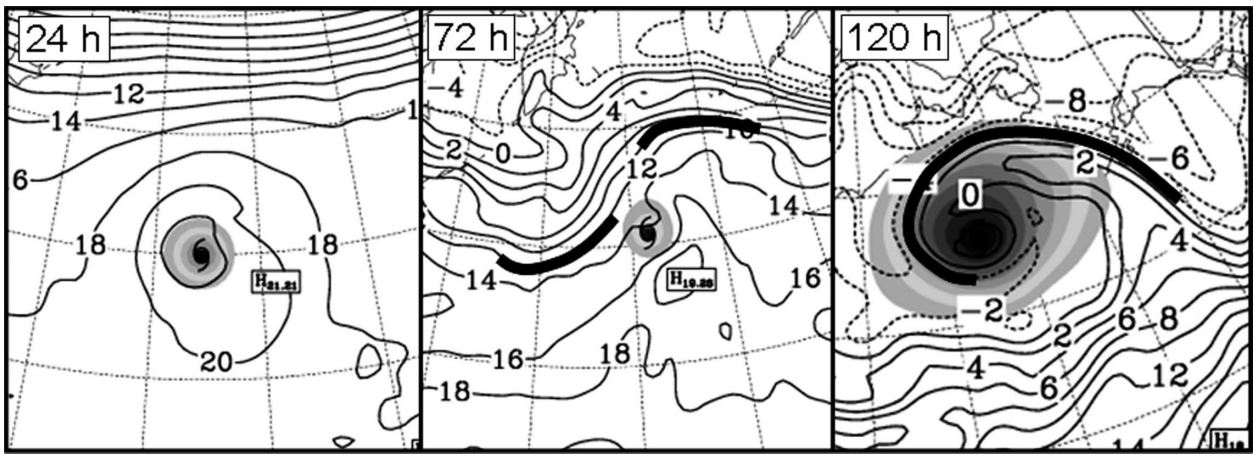

FIG. 6. The 850-mb temperature (contours = 2°C) and SLP (shaded every 4 mb < 1000 mb) within the region indicated by the boxes in Fig. 5 for the intensifying case: (a) 24 h, (b) end of stage 1, and (c) end of stage 2. Frontal zones are indicated with thick lines.

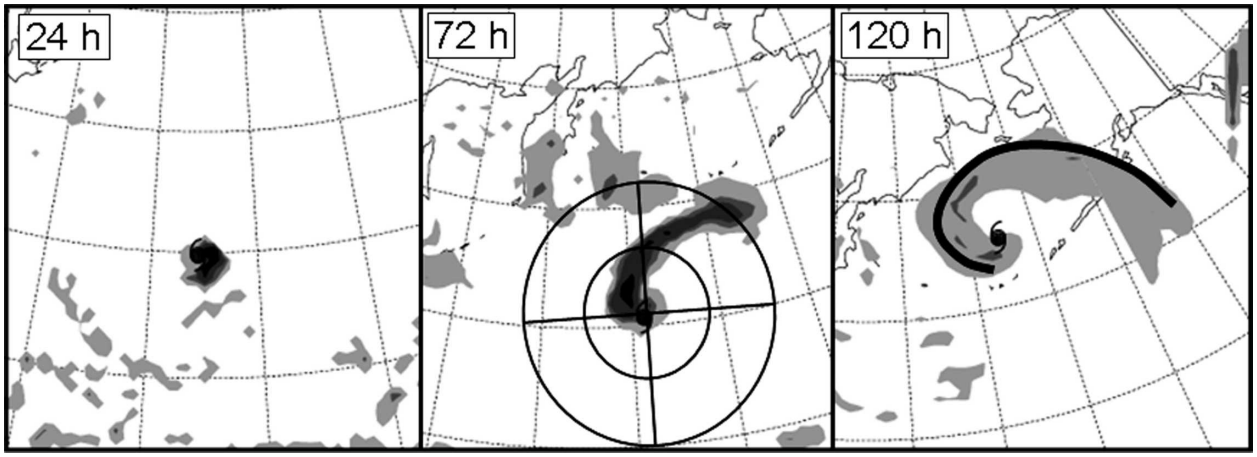

FIG. 7. The 6-hourly precipitation [shading >1 mm (6 h)$^{-1}$, contours 1, 5, 10, 25, 50 mm (6 h)$^{-1}$] within the region indicated by the boxes in Fig. 5 for the intensifying case: (a) 24 h, (b) end of stage 1, and (c) end of stage 2. The circle quadrants in (b) indicate the inner- and outer-quadrant areas that are used to calculate forecast parameters in section 5.

circulation associated with the tropical cyclone has distorted the temperature gradient so that colder (warmer) air has advected to the west (east) of the tropical cyclone center (Fig. 6b). In addition, frontal regions have developed with a strong warm front to the northeast and a weak cold front to the west of the tropical cyclone center. By the end of stage 2 (Fig. 6c), the core of the cyclone is completely surrounded by subfreezing air in a warm seclusion process.

The 6-hourly precipitation maps that correspond to the images in Fig. 5 are presented in Fig. 7. Initially the precipitation is concentrated around the tropical cyclone center and is due to the convective term in the simulation (Fig. 7a). By the end of stage 1 (Fig. 7b), the precipitation is mostly due to the explicit cloud physics scheme and is concentrated in a long arc extending from the tropical cyclone center to the northeast along the warm frontal zone shown in Fig. 6b. Note that very little precipitation is associated with the weak cold front that extends to the west of the tropical cyclone center in Fig. 6b, which seems to be typical of cases in which the tropical cyclone circulation is providing the mechanism for deformation of the baroclinic zone (e.g., Klein et al. 2000). Near the tropical cyclone center, the majority of the precipitation at the end of stage 1 (Fig. 7b) lies in the inner portion of the northwest quadrant and the outer portion of the northeast quadrant, which is typical of the reintensifying cases and is due to the development of precipitation along the warm front from upslope mechanics (e.g., Klein et al. 2000; Ritchie and Elsberry 2003). At the end of stage 2 (Fig. 7c), the precipitation has weakened and is concentrated in a spiral band that extends to the northeast from the cyclone center.

b. Dissipators—Case 25S15E

The 500-mb geopotential height and SLP patterns are presented in Fig. 8 at key stages in the life cycle of a dissipating extratropical transition simulation. Similar to the reintensifying case, the midlatitude trough and the tropical cyclone are initially distinct features in the 500-mb height and surface pressure fields (cf. Figs. 5a, 8a). Prior to 120 h of integration, the tropical cyclone undergoes transformation or stage 1 of extratropical transition (Klein et al. 2000), and weakens considerably as it approaches the midlatitude baroclinic zone with increasing midlatitude vertical wind shear and lower SSTs (Fig. 3). By 120 h (Fig. 8b), the tropical cyclone has become embedded as an open wave on the strong zonal flow that marks the baroclinic zone and has filled to an SLP of 1012 mb (Fig. 3), which would be the end of stage 1 of extratropical transition as defined by Klein et al. (2000). Because the midlatitude trough that was almost directly north of the tropical cyclone in Fig. 8a has moved well to the east of the tropical cyclone in Fig. 8b, no interaction leading to extratropical cyclone development of the remnant TC is possible. By 168 h (Fig. 8c), the tropical cyclone remnants have continued to dissipate until it is barely identifiable as a weak low pressure system.

The 850-mb temperature maps that correspond to the boxed areas in Fig. 8 are presented in Fig. 9. Initially the highest temperatures of 20°–22°C are concentrated near the core of the tropical cyclone (Fig. 9a). The strong temperature gradient associated with the baroclinic zone is well to the north of the tropical cyclone and the thermal trough associated with the midlatitude trough is seen almost directly to the north of the tropi-

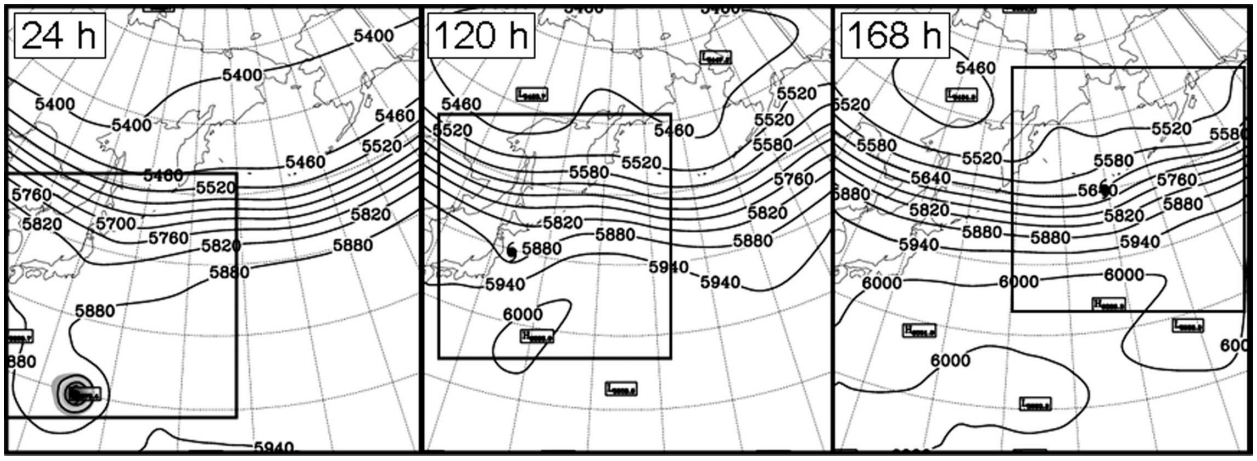

FIG. 8. The 500-mb geopotential height field (contour = 60 m) and SLP (shaded every 4 mb < 1000 mb) for the dissipating case (25S15E): (a) 24 h, (b) end of stage 1 (120 h), and (c) 168 h. The boxes indicate the domains for Figs. 9 and 10.

cal cyclone. By the end of stage 1 of extratropical transition for this simulation (Fig. 9b), the tropical cyclone has moved northward to the edge of the baroclinic zone. However, the tropical cyclone remnants are so weak that only a slight distortion of the zonally oriented baroclinic zone is produced and minimal frontal development is associated with the distortion. By 168 h of integration (Fig. 9c), the tropical cyclone remnants are no longer discernable in the low-level temperature fields.

The 6-hourly precipitation maps that correspond to the images in Figs. 8 and 9 are presented in Fig. 10. Initially (Fig. 10a), the precipitation is concentrated around the tropical cyclone center and is due to the convective term in the simulation, as was the case for the intensifying case (Fig. 7a). By the end of stage 1 (Fig. 10b), the precipitation is mostly due to the explicit cloud physics scheme and is concentrated in two regions: a weak region near the rapidly weakening tropical cyclone, and a broader region with the majority of the precipitation to in the outer northeast quadrant of the tropical cyclone associated with the midlatitude trough, which has advected eastward past the tropical cyclone. This precipitation pattern is typical of the dissipating cases if the upper-level trough has advected to the east of the tropical cyclone remnants (e.g., Klein et al. 2000; Ritchie and Elsberry 2003). In contrast to the intensifying cases, which have a similar pattern of precipitation as the trough and tropical cyclone become phased, more or less precipitation may occur in the northeast quadrant for the dissipating cases depending on how far to the east the trough has advected. When

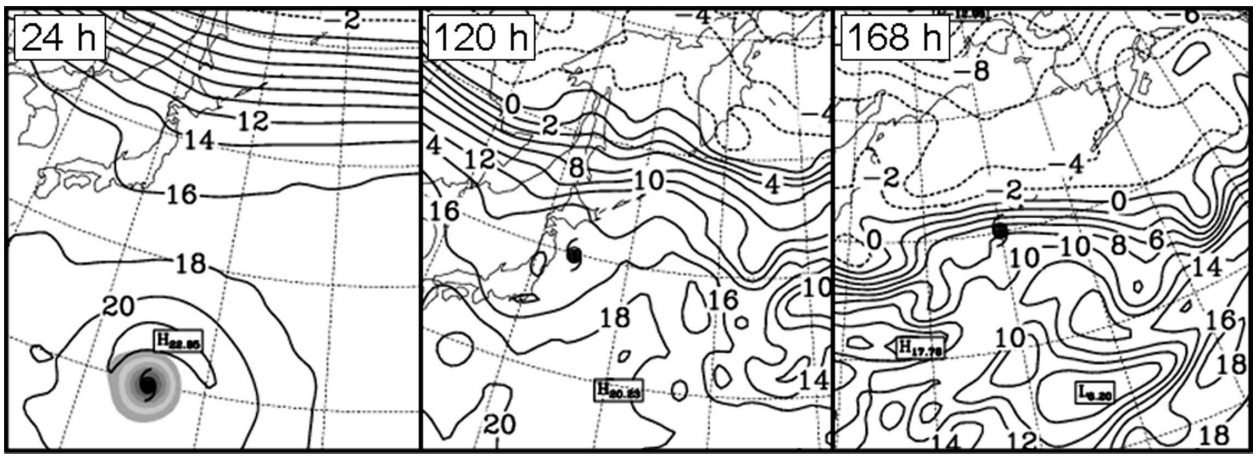

FIG. 9. The 850-mb temperature (contours = 2°C) and SLP (shaded every 4 mb < 1000 mb) within the region indicated by the boxes in Fig. 8 for the dissipating case: (a) 24 h, (b) end of stage 1 (120 h), and (c) 168 h.

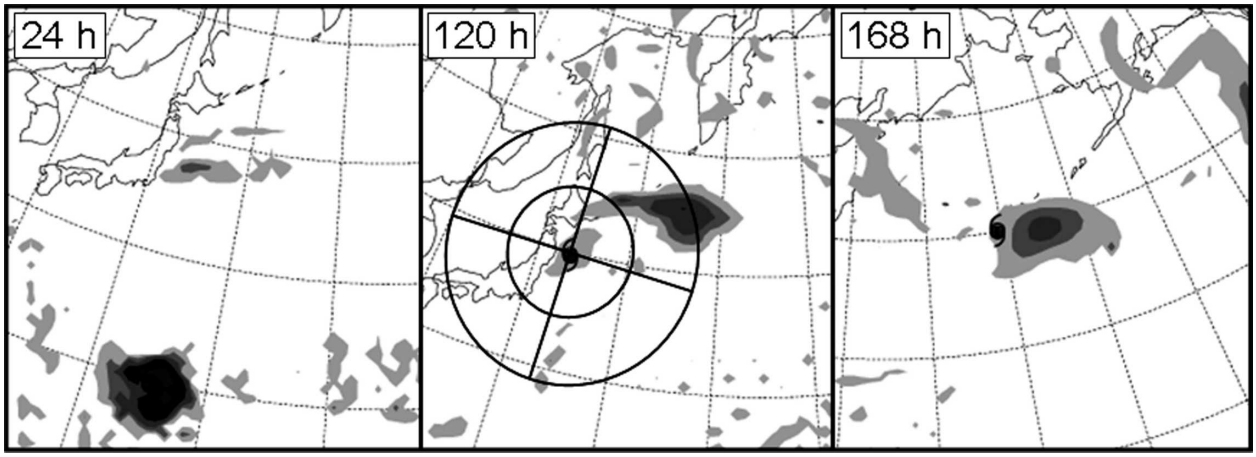

FIG. 10. The 6-hourly precipitation [shading > 1 mm $(6\text{ h})^{-1}$, contours 1, 5, 10, 25, 50 mm $(6\text{ h})^{-1}$] within the region indicated by the boxes in Fig. 8 for the dissipating case: (a) 24 h, (b) end of stage 1 (120 h), and (c) 168 h. The circle quadrants in (b) indicate the inner- and outer-quadrant areas that are used to calculate forecast parameters in section 5.

the tropical cyclone has dissipated (Fig. 10c), the only precipitation is associated with a weak upper-level trough (Fig. 8c), which may have developed in situ with the dissipating tropical cyclone.

5. A discriminating parameter

Because clear differences are simulated in the spatial patterns of certain parameters (e.g., precipitation) depending on whether the tropical cyclone is dissipating or reintensifying, time series of those parameters are constructed to detect these differences ahead of the ET time. The region surrounding the tropical cyclone is split into two annuli: an inner annulus defined as the area within 600 km of the tropical cyclone center, and an outer annulus defined as the annulus from 600 to 1200 km from the tropical cyclone center. These areas are further split into four quadrants: the northeast, northwest, southwest, and southeast quadrants (e.g., Figs. 7b, 10b).

To help identify the discriminating parameters, time series of 500-mb PVA, 925-mb temperature (T) advection, 250-mb divergence and precipitation are constructed relative to their end of the stage-1 point, which is defined as the time of maximum SLP as the tropical cyclone remnants fill prior to reintensification, or as the time (to the nearest 6 h) when the tropical cyclone becomes an open wave in the 500-mb geopotential height field for the dissipating cases. The end of stage 2 is defined as the time of minimum SLP for the reintensifying cases, and is not applicable to the dissipating cases. All cases are plotted on one axis and the time series of inner-quadrant PVA in the northeast and northwest are shown in Fig. 11.

Two clear differences between the intensifying and dissipating cases are shown in Fig. 11. The northeast quadrant, inner-radius (0–600 km), 500-mb PVA is consistently higher prior to the end of stage 1 for intensifying cases than for dissipating cases (Fig. 11a). An approximate threshold value of $25 \times 10^{-10}\ \text{s}^{-2}$ (horizontal line in Fig. 11a) identifies all intensifying cases correctly, and only one dissipating case incorrectly (Table 1) and is 99% significant using a Student's t test. Evaluation of the northwest quadrant, inner-radius 500-mb PVA reveals a distinct rising trend prior to the end of stage 1 to a value of greater than $5 \times 10^{-10}\ \text{s}^{-2}$ (i.e., while the SLP is rising) for intensifying cases versus a decreasing or constant trend of less than $5 \times 10^{-10}\ \text{s}^{-2}$ for the dissipating cases (Fig. 11b). This characteristic correctly identifies all cases as either intensifying or dissipating (Table 1) at a 99% significance level using a Student's t test.

By inspection, 18 main discriminating factors can be discerned prior to the end of stage 1 of the extratropical transition of which 14 tested as significant at a 95% significance level or higher (boldface parameters in Tables 1 and 2). These are the patterns of 500-mb PVA in the inner northeast, inner and outer northwest, and inner southeast quadrants, 200-mb divergence in the inner and outer northwest quadrants, precipitation in the inner and outer northwest quadrants, and the pattern of low-level temperature advection in all inner quadrants and the outer northwest and southwest quadrants of the tropical cyclone (Fig. 12). Some of these are the same patterns that showed clear differences in their spatial patterns between the intensifying and dissipating cases discussed in the previous section.

A physical interpretation based on the Petterssen

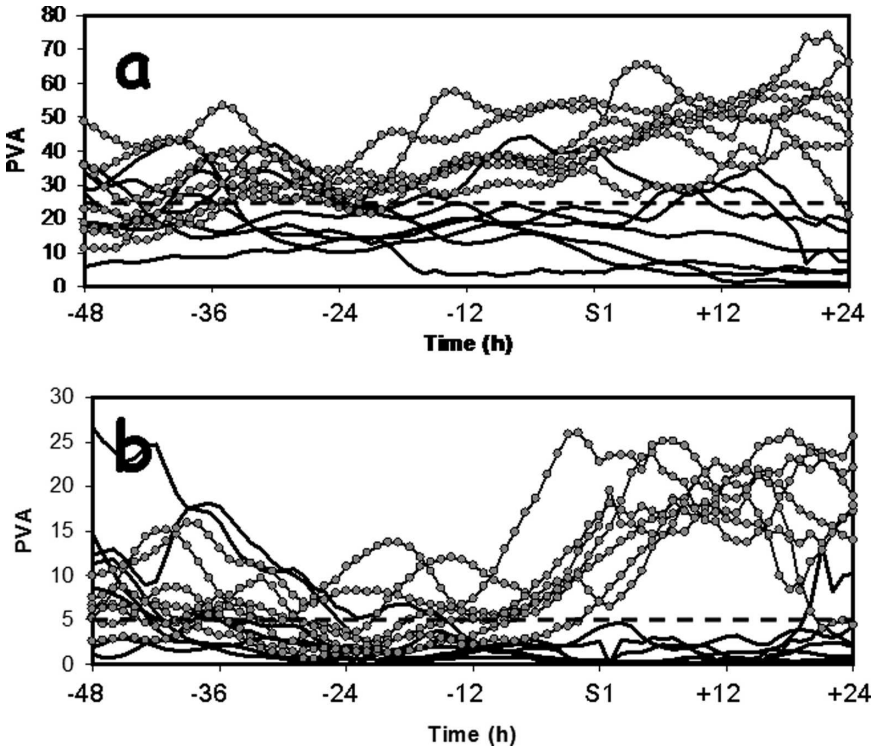

FIG. 11. Time series of intensifying (filled circles) and dissipating (black line) cases adjusted in time relative to the time that stage 1 (S1) is completed for (a) 500-mb positive vorticity advection ($\times 10^{-10}$ s^{-2}) in the northwest quadrant; and (b) total precipitation [mm (6h)$^{-1}$] in the northwest quadrant within 0–600 km. The discriminating value is indicated by the dashed line.

type-B conceptual model is that the reintensifying cases would be experiencing amplification and distortion of the baroclinic zone due to warm advection to the northeast and cold advection to the southwest. This is in conjunction with 500-mb positive vorticity advection in advance of a trough that is tilted westward with elevation due to the cold advection on the west side. Such a trough position is consistent with 200-mb divergence in the northwest quadrant. Significant precipitation in the northwest quadrant is consistent with both the location of an upper-level trough to the west of the tropical cyclone and with enhanced precipitation in the northern sector of the tropical cyclone due to its interaction with vertical shear associated with the increasing west-

TABLE 1. Percentage of intensifier cases (dissipators) correctly (incorrectly) identified by trends in selected parameters in the inner radius prior to the end of stage 1 of ET. Significant differences in the correct detections of intensifiers vs false detection of dissipators are in boldface.

Inner radius 0–600 km (per unit area)	Discriminating value	Intensifiers	Dissipators	Significance (*t* test)
NE: 500-mb PVA	**25×10^{-10} s^{-2}**	**100%**	**14%**	**99%**
NE: 925-mb *T* advection	**7×10^{-5} K s^{-1}**	**100%**	**17%**	**99%**
NE: 200-mb divergence	1.2 c	86%	57%	No
NE: Precipitation	2.3 mm (6 h)$^{-1}$	89%	29%	No
NW: 500-mb PVA	**5×10^{-10} s^{-2}**	**100%**	**0%**	**99%**
NW: 925-mb *T* advection	**9×10^{-10} K s^{-2}**	**100%**	**17%**	**99%**
NW: 200-mb divergence	**0.9×10^{-5} s^{-1}**	**86%**	**14%**	**99%**
NW: Precipitation	**1 mm (6 h)$^{-1}$**	**89%**	**14%**	**99%**
SW: 925-mb *T* advection	**8×10^{-5} K s^{-1}**	**86%**	**17%**	**99%**
SE: 500-mb PVA	**13×10^{-10} s^{-2}**	**72%**	**28%**	**95%**
SE: 925-mb *T* advection	**6×10^{-5} K s^{-1}**	**83%**	**17%**	**99%**

TABLE 2. Percentage of intensifier (dissipator) cases correctly (incorrectly) identified by selected threshold parameters in the outer-radius prior to the end of stage 1 of ET. Significant differences in the correct detection of intensifiers vs false detection of dissipators are in boldface.

Outer radius 600–1200 km (per unit area)	Discriminating value	Intensifiers	Dissipators	Significance (*t* test)
NE: 925-mb *T* advection	5.2×10^{-5} K s^{-1}	71%	33%	No
NE: Precipitation	1.7 mm (6 h)$^{-1}$	100%	43%	No
NW: 500-mb PVA	$\mathbf{2 \times 10^{-10}}$ **s^{-2}**	**100%**	**14%**	**99%**
NW: 925-mb *T* advection	$\mathbf{4 \times 10^{-5}}$ **K s^{-1}**	**86%**	**17%**	**95%**
NW: Divergence	$\mathbf{0.56 \times 10^{-5}}$ **K s^{-1}**	**100%**	**14%**	**95%**
NW: Precipitation	**0.5 mm (6 h)$^{-1}$**	**67%**	**28%**	**95%**
SW: 925-mb *T* advection	$\mathbf{3 \times 10^{-5}}$ **K s^{-1}**	**100%**	**17%**	**99%**

erly midlatitude flow (Ritchie and Elsberry 2001). A number of researchers (e.g., Klein et al. (2000) have identified the development of asymmetric precipitation with a maximum in the northern sector as typical of extratropical transition in the western North Pacific region.

Much stronger signals are present in the stage 2 (re-intensification) parameters (in Table 3). For example, the strong peaks of 850-mb temperature advection in the northeast and southeast quadrants in both the inner and outer radius are clearly different for the intensifying cases than for the dissipating cases and correctly identify all intensifying cases while only incorrectly identifying one dissipating case. However, these parameters change along with an already falling SLP and thus are not of predictive use.

The best use of these parameters is to combine them into a single parameter that indicates whether intensification will or will not occur for any given case of extratropical transition. As a first step, a linear combination of six of the parameters that tested with a significance of 99% up to 6 h prior to the end of stage 1 is developed and examined for its utility in discriminating between intensifying and dissipating cases of ET. The parameters used are inner-quadrant northeast PVA, northwest PVA, northwest temperature advection, and southeast temperature advection, and outer-quadrant north- and southwest temperature advection. Each parameter is normalized by the largest value of that parameter over the entire 16-simulation set, and the linear combination is calculated and plotted from S1 − 48 h to S1 + 24 h in Fig. 13. Note the generally higher values and upward trends prior to S1 for the intensifying cases compared to the dissipating cases. A normalized value of 2.1 discriminates all cases at least 6 h prior to the end of stage 1 and has the advantage of removing concerns

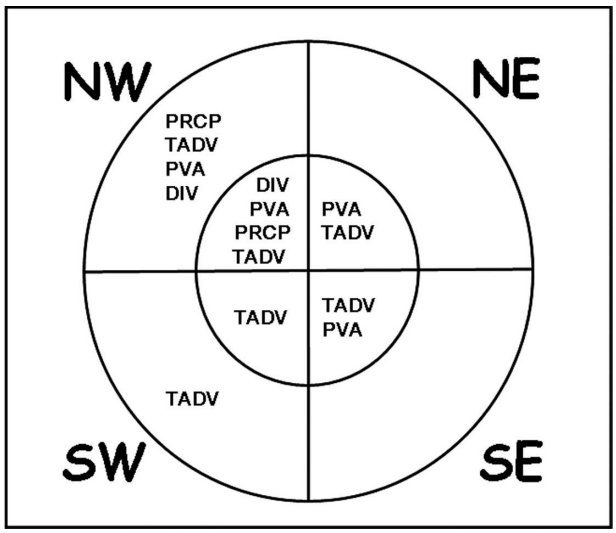

FIG. 12. Quadrants in which discriminating parameters are found prior to the end of stage 1 of the ET that will distinguish between reintensifiers and dissipators. The temperature advection is at 850 mb, the divergence is at 200 mb, and the positive vorticity advection is at 500 mb.

TABLE 3. Percentage of intensifier (dissipator) cases identified by selected threshold parameters during stage 2 of ET.

Inner radius 0–600 km (per unit area)	Discriminating value	Percentage of cases identified after commencement of stage 2	
		Intensifiers	Dissipators
NE: PVA	30×10^{-10} s^{-2}	100%	0%
NE: *T* advection	10×10^{-5} K s^{-1}	100%	17%
NE: Precipitation	4.0 mm (6 h)$^{-1}$	100%	14%
NW: PVA	10×10^{-10} s^{-2}	100%	0%
NW: Divergence	1.8×10^{-5} s^{-1}	100%	14%
NW: Precipitation	2.0 mm (6 h)$^{-1}$	100%	14%
SW: *T* advection	20×10^{-5} K s^{-1}	86%	0%
SE: *T* advection	15×10^{-5} K s^{-1}	100%	17%
Outer radius 600–1200 km (per unit area)			
NE: *T* advection	10×10^{-5} K s^{-1}	100%	0%
NE: Precipitation	0.8 mm (6 h)$^{-1}$	89%	43%
NW: Precipitation	0.23 mm (6 h)$^{-1}$	89%	43%
SW: *T* advection	5×10^{-5} K s^{-1}	100%	0%
SE: *T* advection	9×10^{-5} K s^{-1}	100%	0%

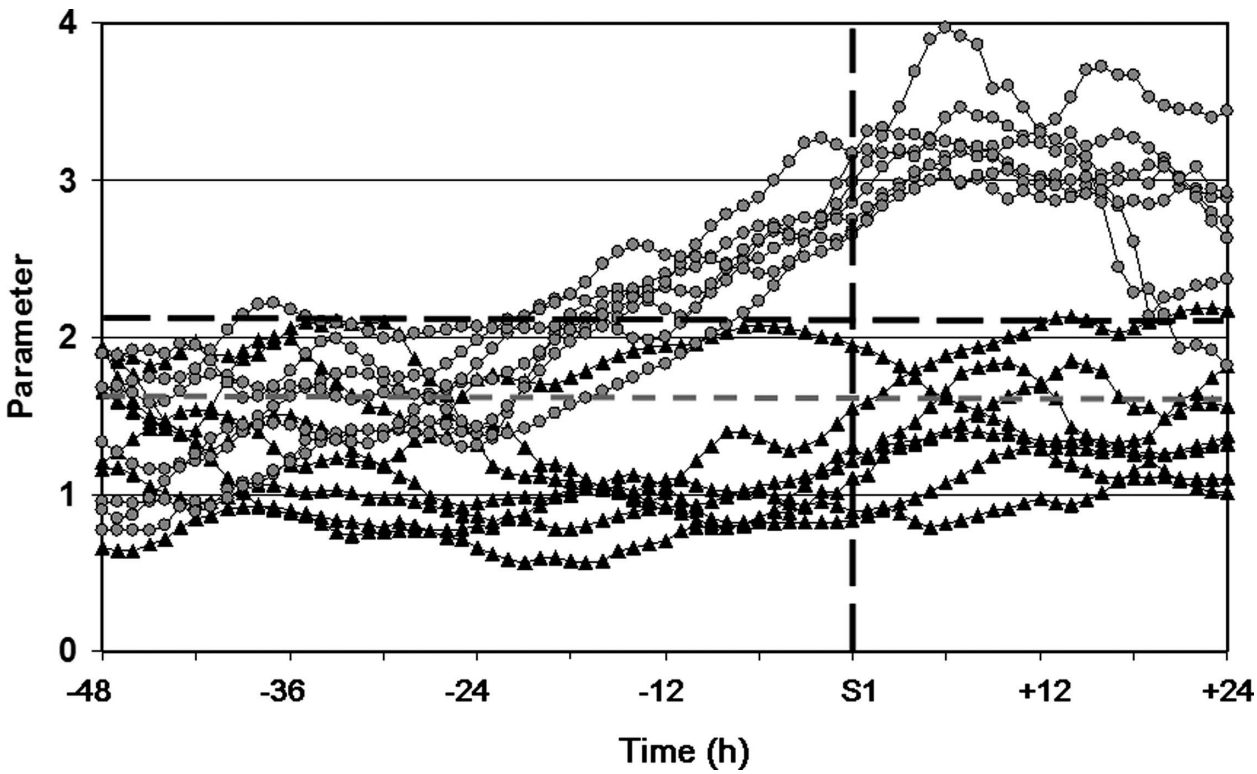

FIG. 13. The linear combination of six normalized discriminating parameters prior to the end of stage 1 of the ET for all 16 simulations. Solid triangles are used for the dissipating cases and gray circles for the intensifying cases. Note the generally higher values and upward trends prior to S1 for the intensifying cases compared to the dissipating cases. A normalized value of 2.1 (heavy dashed line) discriminates all cases at least 6 h prior to the end of stage 1. A normalized value of 1.67 (light dashed line) discriminates all except one case more than 12 h prior to the end of stage 1.

about the absolute value of variables such as precipitation coming out of a gridpoint model. A slightly lower normalized value of about 1.7 would correctly identify all intensifying cases and incorrectly identify one dissipating case as an intensifying case at least 12 h prior to the end of stage 1. Although this result is extremely encouraging, work in progress for developing a robust parameter will involve 1) extending the number of simulated cases to include variations in the trough structure, which will extend the number of cases to 64; and 2) examining real cases using analyses of all the distinguishing parameters for individual cases to validate their usefulness in distinguishing intensifying and dissipating cases

6. Summary and conclusions

Sixteen idealized simulations are used to explore the effects of different phasing between the midlatitude trough and tropical cyclone during extratropical transition. A consistent spatial pattern of strong (S), moderate (M), weak reintensification (W), or dissipation (D) is simulated. Those cases where the tropical cyclone is initially closest (within 15° latitude) to the baroclinic zone and midlatitude trough develop the deepest cyclones and those farthest away (25°S of the trough) are more likely to dissipate or only weakly reintensify. The differences in the interaction between the midlatitude trough and tropical cyclone in these idealized simulations can be related to the phasing of the two systems. Whereas Ritchie and Elsberry (2003) found that the strength of the midlatitude trough had little to do with the peak intensity of the transitioned cyclone, these simulations indicate the peak intensity is extremely sensitive to the initial locations of the two weather systems relative to each other. Work still to be reported indicates that varying the initial strength of the trough along the lines of that accomplished in Ritchie and Elsberry (2003) and repeating the 16-simulation configuration produces little variation in the spatial patterning of S, M, W, and D systems, but the entire pattern shifts closer to or farther from the trough with strength of the trough. We expect that varying the size/strength of the tropical cyclone will also produce some changes in the pattern. Clearly, the main forecasting challenge will be to accurately predict the system positions and the tim-

ing and magnitude of the interaction. Considering the uncertainty in the initial conditions for both systems, and the subtropical ridge that is bringing the tropical cyclone poleward, and the nonlinearity of the interaction this will be a challenging forecast.

Threshold values of various parameters ahead of the end of stage 1 have been identified as being important in distinguishing whether the system was going to reintensify or dissipate. The list of parameters tested included the development parameters of Klein et al. (2000), that is, upper-level divergence, 500-mb positive vorticity advection, and low-level temperature advection, as well as the spatial distribution of precipitation. Fourteen parameters were identified that discriminated between intensifying and dissipating cases of ET *prior to the end of the transformation stage 1* at a significance level of 95% or more. The time series of a simple linear combination of these (normalized) parameters in these simulations demonstrate a capability to discriminate between intensifying and dissipating cases of extratropical transition. However, the caveat is that these parameters have been derived from controlled simulations of ET and their utility in a real forecast situation using operational analyses still needs to be tested. A conceptual model following a Petterssen type-B development scenario with these parameters may be useful to forecasters in assessing the likely validity of the model forecasts.

Future work includes expanding the set of 16 simulations to 64 simulations that include the strong and weak trough cases from Ritchie and Elsberry (2003) as well as varying the translation speed, strength, and size of the tropical cyclone. In addition, the utility of the time series parameters for forecasting will be investigated using analysis fields instead of simulations.

Acknowledgments. The authors would like to acknowledge the insightful comments by Dr. R. Hart and an anonymous reviewer. The COAMPS model was made available by the Naval Research Laboratory, Monterey, CA. Simulations were performed on computers at the Naval Postgraduate School. Postprocessing was achieved using computers located at the Center for High Performance Computing at the University of New Mexico. This research was sponsored by the Office of Naval Research Marine Meteorology Program. Mrs. P. Jones assisted in the preparation of the manuscript.

REFERENCES

Deardorff, J. W., 1980: Stratocumulus-capped mixed layers derived from a three-dimensional model. *Bound.-Layer Meteor.,* **18,** 495–527.

DiMego, M., and L. F. Bosart, 1982: The transformation of tropical storm Agnes into an extratropical cyclone. Part I: The observed fields and vertical motion computations. *Mon. Wea. Rev.,* **110,** 385–411.

Foley, G. R., and B. N. Hanstrum, 1994: The capture of tropical cyclones by cold fronts off the west coast of Australia. *Wea. Forecasting,* **9,** 577–592.

Frank, W. M., and E. A. Ritchie, 2001: Effects of vertical wind shear on hurricane intensity and structure. *Mon. Wea. Rev.,* **129,** 2249–2269.

Harr, P. A., and R. L. Elsberry, 2000: Extratropical transition of tropical cyclones over the western North Pacific. Part I: Evolution of structural characteristics during the transition process. *Mon. Wea. Rev.,* **128,** 2613–2633.

——, ——, and T. F. Hogan, 2000: Extratropical transition of tropical cyclones over the western North Pacific. Part II: The impact of midlatitude circulation characteristics. *Mon. Wea. Rev.,* **128,** 2634–2653.

Harshvardhan, R. Davies, D. Randall, and T. Corsetti, 1987: A fast radiation parameterization for atmospheric circulation models. *J. Geophys. Res.,* **92,** 1009–1015.

Hart, R. E., and J. L. Evans, 2001: A climatology of the extratropical transition of Atlantic tropical cyclones. *J. Climate,* **14,** 546–564.

Hodur, R. M., 1997: The Naval Research Laboratory's Coupled Ocean–Atmosphere Mesoscale Prediction System (COAMPS). *Mon. Wea. Rev.,* **125,** 1414–1430.

Kain, J., and J. M. Fritsch, 1993: Convective parameterization for mesoscale models: The Kain–Fritsch scheme. *The Representation of Cumulus Convection in Numerical Models, Meteor. Monogr.,* No. 46, Amer. Meteor. Soc., 165–170.

Keyser, D., M. J. Reeder, and R. J. Reed, 1988: A generalization of Petterssen's frontogenesis function and its relation to the forcing of vertical motion. *Mon. Wea. Rev.,* **116,** 762–780.

Klein, P. M., P. A. Harr, and R. L. Elsberry, 2000: Extratropical transition of western North Pacific tropical cyclones: An overview and conceptual model of the transformation stage. *Wea. Forecasting,* **15,** 373–395.

——, ——, and ——, 2002: Extratropical transition of western North Pacific tropical cyclones: Midlatitude contributions to intensification. *Mon. Wea. Rev.,* **130,** 2240–2259.

Louis, J. F., 1979: A parametric model of vertical eddy fluxes in the atmosphere. *Bound.-Layer Meteor.,* **17,** 187–202.

McBride, J. L., and R. M. Zehr, 1981: Observational analysis of tropical cyclone formation. Part II: Comparison of nondeveloping versus developing systems. *J. Atmos. Sci.,* **38,** 1132–1151.

McTaggart-Cowan, R., J. R. Gyakum, and M. K. Yau, 2001: Sensitivity testing of extratropical transitions using potential vorticity inversions to modify initial conditions: Hurricane Earl case study. *Mon. Wea. Rev.,* **129,** 1617–1636.

Perkey, D. J., and C. W. Krietzberg, 1976: A time-dependent lateral boundary scheme for limited-area primitive equation models. *Mon. Wea. Rev.,* **104,** 744–755.

Petterssen, S., 1956: *Weather Analysis and Forecasting.* 2d ed. Vol. I, McGraw-Hill, 428 pp.

——, and S. J. Smebye, 1971: On the development of extratropical cyclones. *Quart. J. Roy. Meteor. Soc.,* **97,** 457–482.

Ritchie, E. A., and R. L. Elsberry, 2001: Simulations of the transformation stage of the extratropical transition of tropical cyclones. *Mon. Wea. Rev.,* **129,** 1462–1480.

——, and ——, 2003: Simulations of the extratropical transition of tropical cyclones: Contributions by the midlatitude upper-

level trough to reintensification. *Mon. Wea. Rev.,* **131,** 2112–2128.

Rutledge, S. A., and P. V. Hobbs, 1983: The mesoscale and microscale structure of organization of clouds and precipitation in midlatitude cyclones. VIII: A model for the "seeder-feeder" process in warm-frontal rainbands. *J. Atmos. Sci.,* **40,** 1185–1206.

Sinclair, M. R., 1993: Synoptic-scale diagnosis of the extratropical transition of a southwest Pacific tropical cyclone. *Mon. Wea. Rev.,* **121,** 941–960.

——, 2002: Extratropical transition of southwest Pacific tropical cyclones. Part I: Climatology and mean structure changes. *Mon. Wea. Rev.,* **130,** 590–609.

Thorncroft, C., and S. C. Jones, 2000: The extratropical transitions of Hurricanes Felix and Iris in 1995. *Mon. Wea. Rev.,* **128,** 947–972.